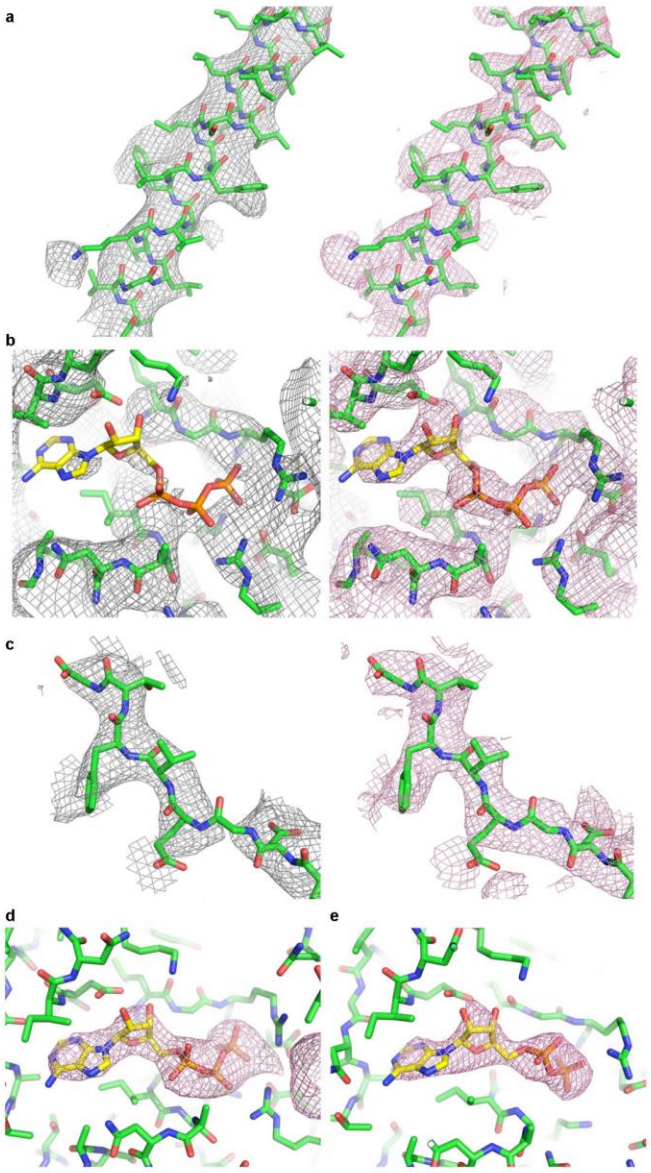

Supplementary Figure 1. Electron density maps. Pre-averaged (left) and averaged maps (right) of different KtrAB regions (1σ contour): **a)** M1 helix in repeat D2 of a KtrB subunit, **b)** ATP bound to KtrAB, **c)** C-terminus of a KtrB subunit. Pre-averaged maps were calculated with 5Å final model phases. Averaged maps were calculated after 4-fold and 8-fold averaging and phase extension from 5.0 Å to 3.5Å. Simulated-annealing fo-fc omit maps (3σ contour) of ligand binding site in the **d)** KtrA-ATP and **e)** KtrA-ADP ring structures. Annealing was performed in a model without ligand.

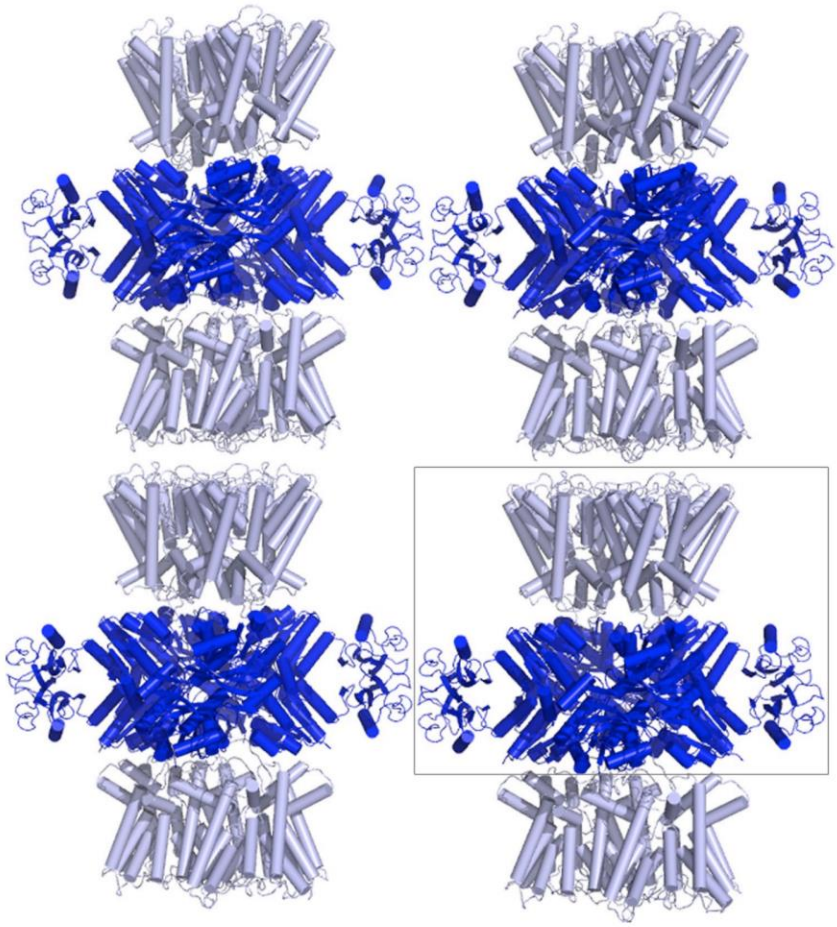

Supplementary Figure 2. Representation of lattice in KtrAB crystals. KtrB homodimers are shown in light blue and KtrA rings in dark blue. A KtrAB complex is delimited by box. Contents of asymmetric unit correspond to the KtrB homodimer and KtrA ring contained within box plus the KtrB homodimer observed below the box in an inverted position.

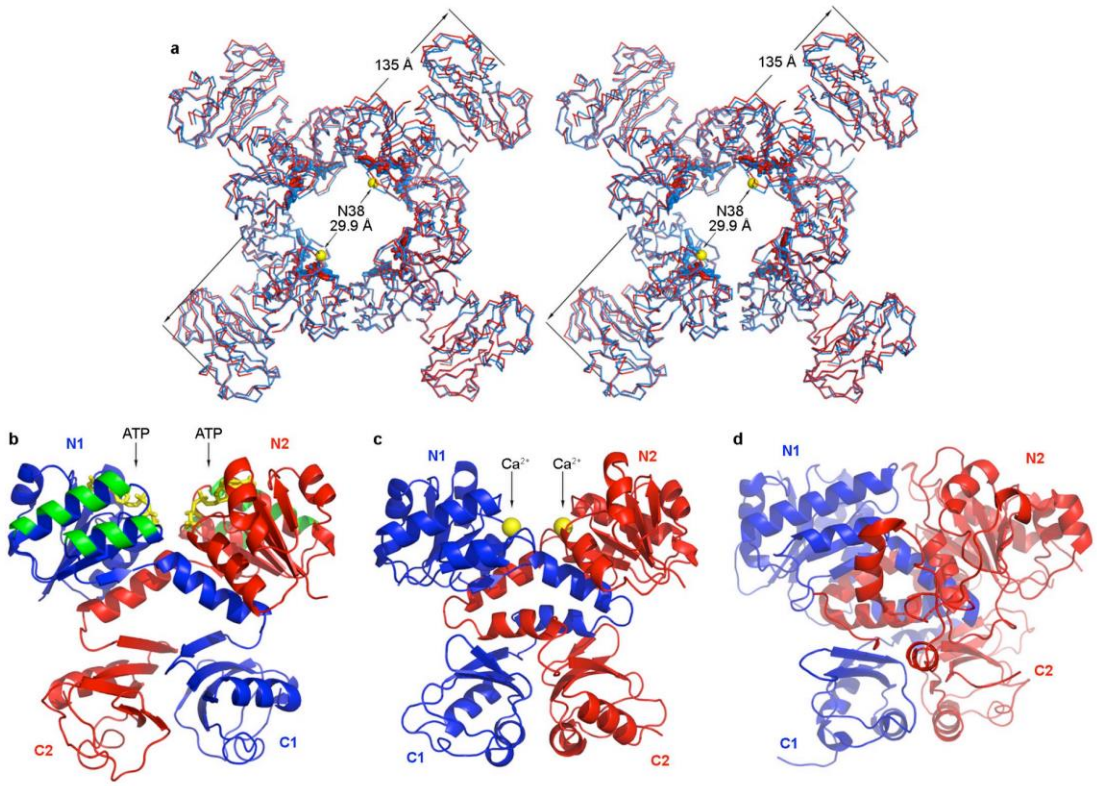

Supplementary Figure 3. KtrA structure. **a)** Stereo-view of superposition of the 4-fold octameric square rings of KtrA from the KtrAB-ATP complex structure (in blue) and from the isolated KtrA-ATP structure (in red). One of the dimensions of the ring from the KtrAB complex is indicated, together with the distance separating N38 Cα in opposite subunits (for comparison with previously published structures of truncated KtrA[21]). RCK dimers from **b)** KtrA, **c)** MthK K^+ channel (PDB code: 1LNQ) **d)** Large-conductance Ca^{2+}-gated K^+ (BK) channel (PDB code: 3NAF). Pairs of sequential lobes are shown in red (N1-C1) and blue (N2-C2). ATP molecules or Ca^{2+} ions are shown in yellow. Surface regions involved in dimer-to-dimer interfaces within the KtrA octameric ring are colored in green. The KtrA dimer is formed by two identical polypeptides. The two subunits undergo a domain-swap and the C-lobe of one subunit ends on the opposite "side" of the dyad relative to its N-lobe. In the MthK channel, a polypeptide spans a channel subunit plus one of the RCK domain, while a separate polypeptide encodes the other RCK domain alone. Domain-swap also happens in MthK but the C-lobe of a subunit stays on the same side as its N-lobe. This is due to the presence of an extra helix at the N-terminal end of the C-lobe which "crosses" the dyad again. In the BK channel, a channel subunit plus the two RCK domains shown form a single polypeptide. Although there are extra-protein regions, the organization of N- and C-lobes resembles more what happens in the MthK channel than in KtrA.

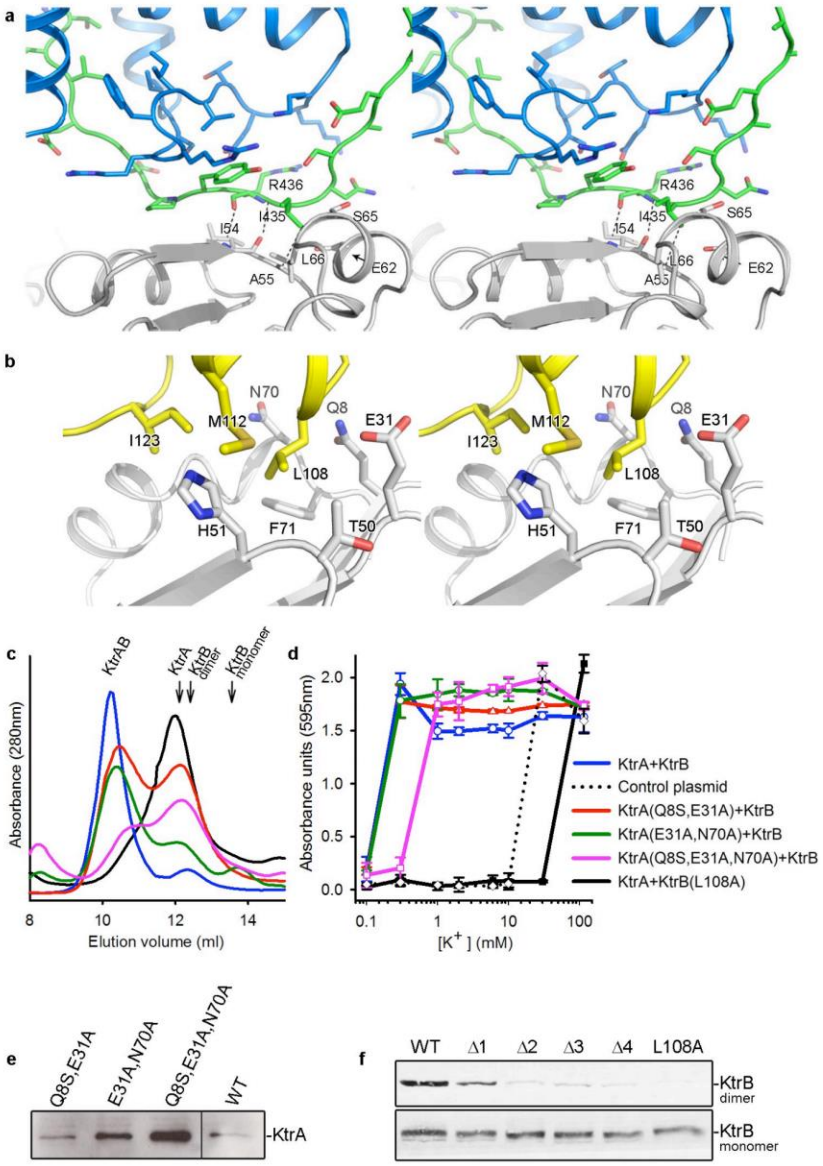

Supplementary Figure 4. Interface regions in the KtrAB complex. See also Supplementary Discussion. **a)** Stereo-view of a lateral-contact region formed between D3-D4 loop of a KtrB subunit (in blue), a stretch of the C-terminus of the neighbouring KtrB subunit (in green) and a KtrA subunit (in gray). Side chains are shown as stick; dashed lines indicate interactions between residues. **b)** Stereo-view of tip-contact region. Residues in D1-D2 KtrB loop (yellow ribbon and stick) interacting with the surface of a KtrA subunit (in white). **c**) Superposition of size-exclusion chromatography elution profiles of wild-type KtrAB and mutant KtrAB (assembled from different KtrA or KtrB mutants and wild-type counterparts). Mixtures were performed at the same concentrations and same ratios. Color coding of curves is indicated at the right of panel d). Elution volumes for KtrAB, KtrA (octamer) and KtrB (monomer and dimer) are indicated. **d)** Plot of bacterial culture optical density as a function of K^+ concentration. TK2420 strain,

transformed with a dicistronic plasmid co-expressing wild-type KtrB with KtrA, or KtrB with KtrA double or triple mutants (as indicated), or KtrB L108A with wild-type KtrA, were grown for 15h before measurement of optical densities. Control plasmid corresponds to bacteria transformed with empty plasmid. Each curve is an average measurement of 3 independent experiments initiated from different colonies; error bars indicate standard deviation of error. **e)** Western blot of soluble fraction of TK2420 lysates probed with anti-KtrA antibody. Lysates were prepared from TK2420 cells expressing wild type KtrB together with wild type KtrA or KtrA mutants (Q8S/E31A, E31A/N70A or Q8S/E31A/N70A). **f)** Western blot of membrane fraction probed with anti-KtrB antibody.A membrane fraction was prepared from BL21(DE3) strain over-expressing wild type KtrB or KtrB mutants (L108, Δ1, Δ2, Δ3, or Δ4). The Δ mutants correspond to sequential truncations of the C-terminus and are described in the main text and in Figure 2. Bands corresponding to dimeric KtrB are more visible in some lanes.

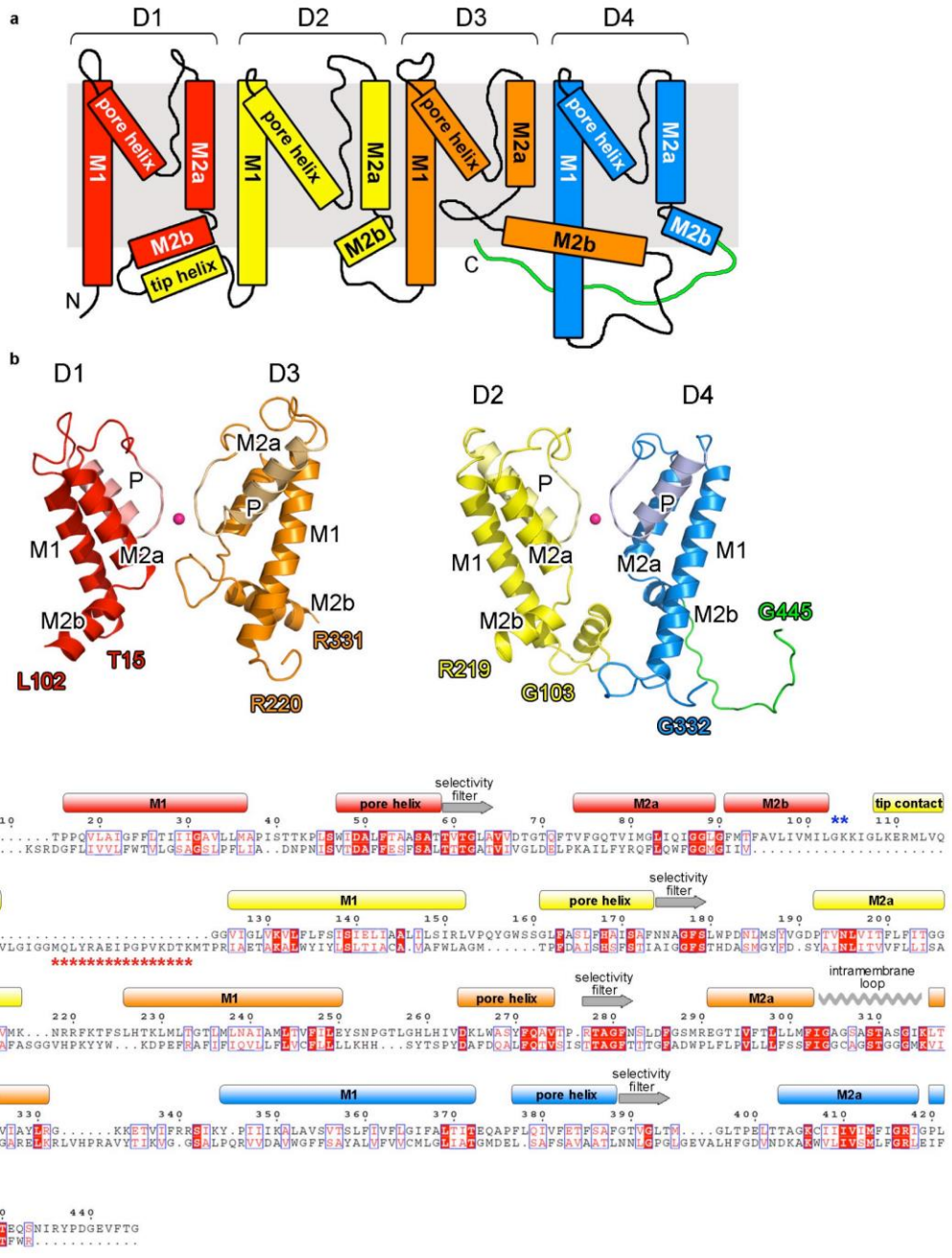

Supplementary Figure 5. KtrB subunit. **a)** Topology diagram of KtrB subunit structure. Repeats are colored differently. **b)** Two views of the 4 repeats forming a KtrB subunit. Only pairs of opposing repeats are presented in each view, namely D1 and D3 (left) and D2 and D4 (right). M1, P, M2a and M2b labels indicate helices in repeats. Repeats are colored differently, with an equivalent paler color for the pore helix (P). C-terminus tail of subunit is show in green. N- and C-terminal residues of each repeat are indicated. Extracellular face of the protein is at the top of the figure. **c)** Pair-wise structural sequence alignment of *B.subtilis* (Bs) KtrB and *V.parahaemolyticus* (Vp) TrkH (PDB code: 3PJZ) as calculated by the program STRAP[39] and represented using ESPript[40]. Repeats are shown with same colors as in a).

Structural features of KtrB are indicated: colored cylinders represent helices, gray arrows the selectivity filter stretches and zigzag line the intramembrane loop. Helix establishing tip-contact is also shown. Residues that are not structurally ordered, and therefore not defined, in the structure are indicated by stars (blue for KtrB; red for TrkH) positioned above the KtrB sequence or below the TrkH sequence.

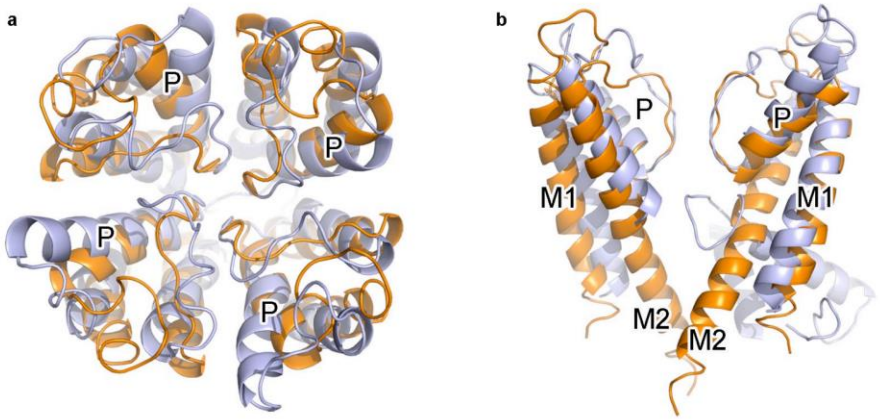

Supplementary Figure 6 Superposition of KtrB subunit and K^+ channel pore. **a)** Extracellular view and **b)** side-view (extracellular face at top of figure) of superposition of the structures of a KtrB subunit (in light blue) and the KcsA potassium channel (PDB code: 1BL8) in orange. Superposition was done through the final four residues in the pore helices and the first two residues in each selectivity filter sequence. Pore helices (P) and the M1 and M2 helices of channel are indicated. This superposition shows that the extracellular halves of the molecules are similar, with just relatively small adjustments in the packing of the helices and a widening of the pore opening. In contrast, the cytoplasmic regions are more divergent, particularly due to the short span of the M2a helix and the presence of the M2b helix in KtrB.

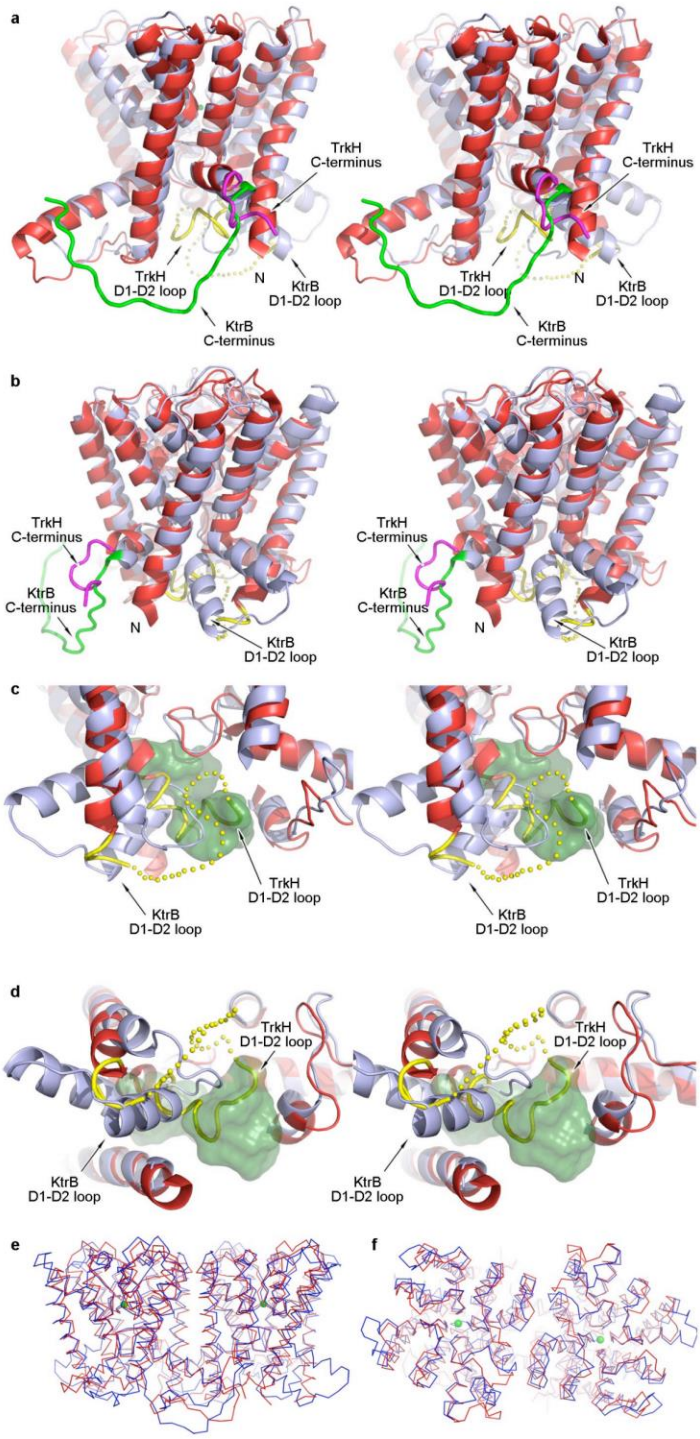

Supplementary Figure 7. Superposition of the structures of *B.subtilis* KtrB and *V.parahaemolyticus* TrkH (PDB code: 3PJZ). **a)** and **b)** Two stereo-views, related by a 90° rotation along the central axis of the molecules, of superposition of a subunit of KtrB (light-blue) and TrkH (red). C-termini are shown in green for KtrB and in magenta for TrkH. TrKH region corresponding to M2b-helix/D1-D2 loop is shown in yellow with dotted line representing a missing stretch. D0 domain from TrkH (~residues 1-64), which

is absent in KtrB, has been removed for clarity. **c)** and **d)** Stereo-views, related by a 90° rotation, of the cytoplasmic faces of the superposed KtrB and TrkH molecules. Helices M2a and M2b of repeat D2 as well as helix M1 of repeat D3 were removed for clarity. Colors as in a) and b). Surface representation of the ion pathway of KtrB (in green) was calculated with program Hollow[41] using a 1.4 Å probe radius. D1-D2 loops are indicated and labeled as in a) and b). Dotted line represents a missing stretch of TrkH D1-D2 loop. **e)** Side-view and **f)** extracellular view of superposition of the homodimeric structures of KtrB (blue) and TrkH (red), shown as Cα traces. K^+ ions are represented by green spheres.

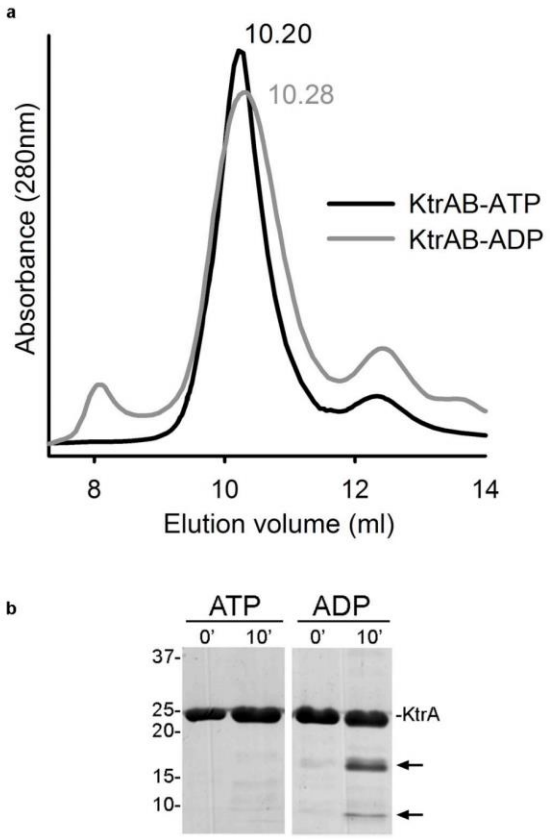

Supplementary Figure 8. Biochemical experiments. **a)** Superposed size-exclusion elution profiles of wild type KtrAB complexes assembled in the presence of ATP or ADP showing no major differences. **b)** Time course of controlled-proteolysis experiment with trypsin added to purified KtrA-ATP or KtrA-ADP (at 1:50 w/w ratio). Reaction was stopped by addition of SDS sample buffer and boiling and aliquots were run in an SDS-PAGE. Increased protease sensitivity of ADP bound protein relative to KtrA-ATP is revealed by the emergence of smaller molecular weight bands (indicated by arrows). This difference is indicative of a conformational difference in solution between the two KtrA forms. Bakker and colleagues[20] showed a similar result for KtrA from *V.alginolyticus* bound to ATP and ADP.

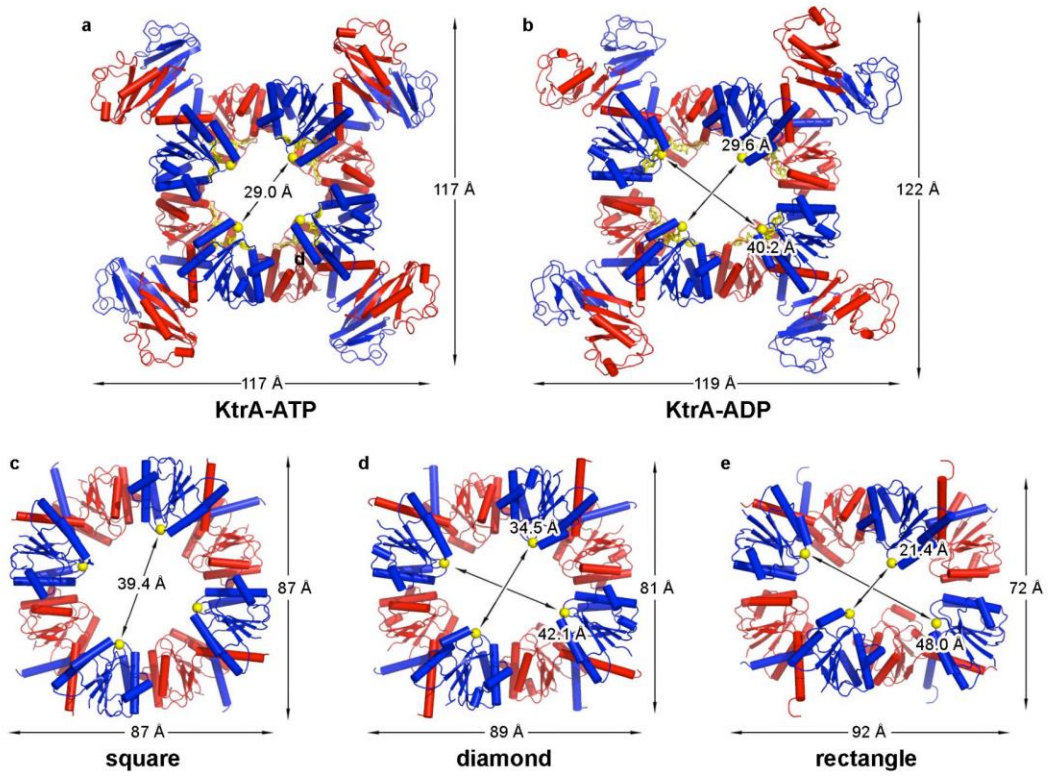

Supplementary Figure 9: KtrA structures. Structures of isolated full-length KtrA with **a)** bound ATP or **b)** with bound ADP. Structures of truncated KtrA (without C-lobe): **c)** in the square conformation (PDB code: 2HMW), **d)** in the diamond conformation (PDB code: 2HMU) and **e)** in the rectangle conformation (PDB code: 2HMS). Alternate subunits are shown in red and blue. Overall dimensions of rings are shown as well as the distance separating N38 Cα from opposite subunits. This simple analysis shows that the conformations of KtrA-ATP and KtrA-ADP are different from the conformations adopted by truncated KtrA and therefore that the RCK domain C-lobe affects the structural properties of the ring.

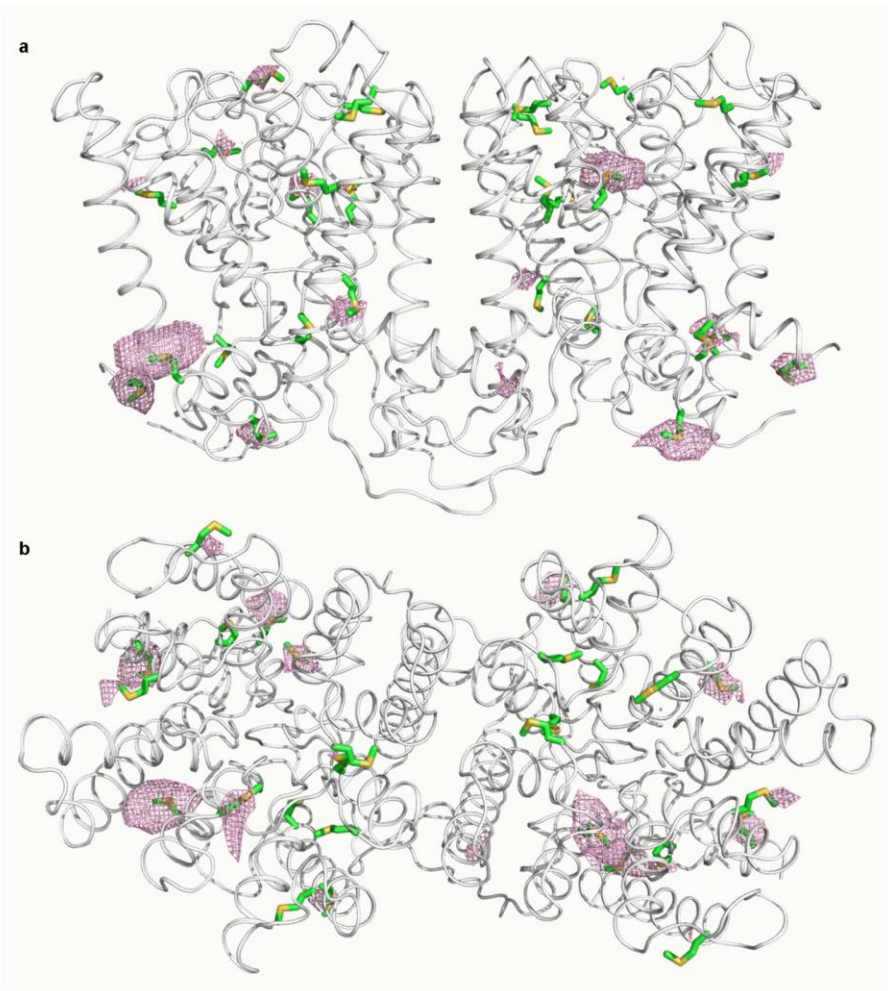

Supplementary Figure 10. Anomalous difference map for selenomethionine-substituted KtrB in complex with KtrA-ATP. Side-view (top) and extracellular view of the KtrB homodimer, shown as Cα trace. Anomalous difference map is contoured at 3.2σ; anomalous difference peaks were considered reliable if present above 3.5σ. Methionines are shown as stick. Selenomethionine substituted KtrB was assembled with KtrA-ATP and crystallized. Map was calculated with anomalous differences to 7.4Å and model phases. The phases were obtained after molecular replacement using the KtrB and KtrA-ATP structures as search models followed by TLS refinement in PHENIX[34].

Supplementary Table 1

Crystal	KtrAB		KtrA-ATP	KtrA-ADP
Space group	$P2_1$		I4	C2
Cell dimensions				
a, b, c (Å)	146.5, 140.2, 153.9		122.8,122.8, 84.1	147.9,84.6, 113.7
α, β, γ (°)	90, 105.7, 90		90, 90, 90	90, 128.4, 90
Diffraction statistics	**Before anisotropic correction**	**After anisotropic correction**		
Resolution (Å)	43-3.30 (3.48-3.30)	43-3.30* (3.49-3.30)	40-3.10 (3.26-3.10)	43-2.78 (2.93-2.78)
No. unique reflections	87633 (12693)	61449 (950)	11441 (1645)	27727 (4004)
No. measured reflections	200097 (27187)		40388 (5849)	134958 (19307)
Multiplicity	2.3 (2.1)		3.5 (3.6)	4.9(4.8)
Completeness (%)	97.2 (97.2)	68.3 (7.0)	99.6 (99.6)	99.7 (99.7)
I/σI	4.5 (0.6)		12.2 (0.9)	12.5 (0.9)
Rsym (%)	16.3 (134.7)		5.2 (83.9)	5.3 (82.7)
Refinement statistics				
Resolution range (Å)	43-3.5 (3.59-3.5)		40-3.24 (3.32-3.24)	43-2.93 (3.00-2.93)
No. reflections	57311		9564	22599
Rwork/Rfree (%)	25.9/27.3 (30.2/31.8)		19.0/24.0 (32.5/31.0)	25.2/27.8 (35.6-41.4)
Total No. of atoms	26564		3479	6634
No. of waters	0		3	0
No. of ATP	8		2	0
No. of ADP	0		0	4
No. of K^+	4		0	0
Chain average *B*-factor				
KtrB subunits	52-63			
KtrA subunits	58-82		80-86	56-66
ATP or ADP molecules	28-43		96-98	60-74
K^+	27			
waters			80	
R.m.s. deviations				
Bond lengths (Å)	0.008		0.007	0.011
Bond angles (°)	1.39		1.14	1.35

The values in parenthesis correspond to statistics for data in the highest resolution shell. *Recommended resolution limits after anisotropic correction are 3.8, 4.1 and 3.3Å, respectively along a*, b* and c* reciprocal space directions. We have, however, decided to refine the model against data to 3.5Å since there was no visible improvement in refinement statistics or map quality with data to the recommended limit.

Supplementary discussion

Interaction regions between KtrB homodimer and the KtrA ring

The interactions observed in the KtrAB complex between KtrB and the KtrA ring, the lateral-contact and tip-contact regions (Figure 1c, 1d), are a major difference relative to potassium channels, where interaction is mostly dependent on a peptide linker connecting the channel region and the RCK ring.

In KtrAB the lateral-contact regions involve part of the KtrB C-terminus (Figure 1c, 1d). The 18 residue long C-terminus of each KtrB subunit runs along the homodimer interacting extensively with the neighboring KtrB subunit. Residues 434 to 438 in the C-terminus mediate all the KtrB/KtrA interactions in this contact and are sandwiched (Supplementary Figure 4a) between the KtrB cytoplasmic loop connecting repeats D3 to D4 and the KtrA surface. The ~660 $Å^2$ of buried surface area include main-chain interactions between KtrB R436 and KtrA I54 and contacts between KtrB I435 and several KtrA residues: L66, E62, S65 and A55.

The tip-contact regions occur at the apexes of the cytoplasmic face of the KtrB homodimer (Figure 1a, 1c, 1d) where the KtrB cytoplasmic loops connecting repeats D1 and D2 interact with two opposing KtrA subunits, each contact burying a total surface area of ~850 $Å^2$. The D1-D2 loop encompasses residues 103 to125 and adopts a helical conformation over residues 108 to 117 (Figure 1d). The interaction (Supplementary Figure 4b) involves hydrogen-bonding between KtrA residues (Q8, E31 and N70) and KtrB main-chain and side-chain atoms, as well as a network of Van der Waals contacts involving L108, M112 and I123 in KtrB and T50, H51 and F71 in KtrA.

To demonstrate the functional relevance of the interactions present in the *in vitro* assembled complex we mutated several residues in the tip-contact (Q8S/E31A, E31A/N70A and Q8S/E31A/N70A in KtrA and L108A in KtrB) and evaluated their impact *in vitro*, on the assembly of KtrAB, and *in vivo*, using a previously described growth complementation assay[3,6,8]. The complementation assay makes use of the *E.coli* TK2420 strain, which has its major K^+ transport systems disabled and only grows in K^+ concentrations above 30 mM; expression of wild-type KtrAB allows growth to occur in low K^+ concentrations (~0.3 mM) while KtrB alone does not rescue growth.

Size-exclusion chromatography profiles reveal that, just like in a typical protein-protein interaction, many of the interface residues (Q8S, E31A and N70A) have a relatively small impact on complex stability, while L108A behaves as a hotspot and affects drastically the assembly of KtrAB (Supplementart Figure 4c). Importantly, the KtrB L108A mutant still forms homodimers, indicating that KtrB folding is not affected by the mutation. Consistently, the assembly-deficient L108A transporter mutant does not rescue TK2420 growth while the other mutants do (Supplementary Figure 4d).

Failure in complementing growth of the TK2420 strain could result from a drastic drop in the expression levels of the protein mutants. We have found that this is not happening with any of our mutants, therefore supporting our functional interpretation of the results. The expression levels of the KtrA mutants were equivalent or higher than wild type protein, as evaluated by western blot analysis of TK2420 cells extract (Supplementary Figure 4e). Wild type KtrB is expressed at very low levels in our complementation assay and is not detectable. Therefore, impact of KtrB mutations on protein levels was evaluated by western blot analysis of membrane preparations from the over-expression system, also used for the biochemical and crystallographic work. A blot shows that L108A (which does not complement the TK2420 growth assay) had a minimal effect, a decrease of ~2-fold, on the level of KtrB protein in the membrane

(Supplementary Figure 4f). Importantly, this level is very similar to the protein levels of other KtrB mutants (mutants Δ1, Δ2 and Δ3 in the KtrB C-terminus – see main text and Figure 2) that are fully functional in the complementation assay.

Overall, these results demonstrate that the protein-protein contacts observed in our KtrAB crystal are functionally relevant, supporting, therefore, the structural and functional significance of our *in vitro* assembled KtrAB complex.

Discussion of ligand dependent activation models in KtrAB

The models we have proposed for activation of KtrAB have as the central feature the activation of the transporter upon ligand binding and contraction of the KtrA (RCK) ring. This is clearly different from what has been proposed for channel gating by RCK rings, where channel activation is the result of ring expansion. This difference only appears to be mechanistically incompatible since it can be easily resolved by the mode by which the change in the RCK ring is coupled to the changes in the channel or transporter gates. This apparent incompatibility is not dissimilar to what happens in the voltage-gating mechanisms of HCN (hyperpolarization-activated cyclic nucleotide-gated) and Kv (voltage-gated potassium) channels. In voltage-gated channels the movement of the voltage sensor across the membrane in response to voltage changes is most likely identical in HCN and Kv channels but the functional consequences are opposite; upon membrane hyperpolarization the inward movement of the voltage sensor causes HCN channels to open, while it causes Kv channels to close. For further information on voltage-gating in HCN and Kv channels see a recent commentary by Mark Trudeau[27] and references within.

How could contraction of the RCK ring lead to activation of transport? We can imagine a simple mechanism where the ring conformational change results in engagement and disengagement of some of the interactions established with the KtrB homodimer, without affecting complex stability. So, in the expanded KtrA ring (with bound ADP) there is a disengagement of some of these interactions, allowing for the relaxation of the KtrB conformation and the adoption of a closed conformation. Upon binding of ATP, the KtrA ring contracts and there is a re-engagement of the contacts, leading to a conformational change in KtrB, adoption of the KtrAB conformation present in our structure, opening of the gate and an increase in transporter activity. Interestingly, a mechanism involving engagement and disengagement of different protein regions has been proposed for gating of the pentameric ligand-gated ion channels[28].